
Logic-inspired Deep Neural Networks

Minh Le¹

Abstract

Deep neural networks have achieved impressive performance and become de-facto standard in many tasks. However, phenomena such as adversarial examples and fooling examples hint that the generalization they make is flawed. We argue that the problem roots in their distributed and connected nature and propose remedies inspired by propositional logic. Our experiments show that the proposed models are more local and better at resisting fooling and adversarial examples. By means of an ablation analysis, we reveal insights into adversarial examples and suggest a new hypothesis on their origins.

1. Introduction

The success of ReLU-based networks in recent years originates from their *learnability* and *expressiveness*. Their piecewise linearity character helps them avoid gradient exploding or vanishing problems of early architectures (Hochreiter et al., 2001). In terms of expressive power, it has been shown that they are capable of capturing an exponential amount of variations (Raghu et al., 2017; Montúfar et al., 2014).

However, little can be guaranteed about the *validity* of the learned representations. Recent work has shed light on two troubling phenomena: adversarial examples (Szegedy et al., 2013) and fooling examples (Nguyen et al., 2015). The former, in image recognition, are images slightly perturbed to fool a model while being semantically the same to human eyes. The latter, fooling examples, are images that do not belong to any class and yet are classified to one with high confidence. Both the results of Szegedy et al. (2013) and Nguyen et al. (2015) demonstrate that a model that is easy to train can also easily make invalid generalizations.

Much research has been devoted to explaining these phenomena since (Goodfellow et al., 2014; Moosavi-Dezfooli et al., 2017; Ford et al., 2019). Recently, Nguyen et al.

$x_{0,1}$	$x_{0,2}$	\dots	$x_{m,n}$	c_1	c_2	c_3
0	0	\dots	0	0	0	0
0	0	\dots	1	1	0	0
\vdots	\vdots	\ddots	\vdots	\vdots	\dots	\vdots
1	1	\dots	1	0	0	1

Figure 1. The classification of binary images can be viewed as the problem of completing a truth table in which inputs are pixels and outputs class memberships.

(2018) identifies the tendency of ReLU networks to create connected classification regions as a likely source of the lack of validity of certain models.

We identify its distributed nature as a potential source of fooling examples. ReLU activation is stronger the *further* the input is from its decision boundary. Fooling examples are typically far from decision boundaries (for example, Gaussian noise can often fool deep neural networks) and therefore also likely to receive a high signal from the network. A more principled approach would be to make a *local* and *smooth generalization* in which a model makes confident predictions within bounded regions of the input space and gradually become less confident further away.

Logic propositions represent a class of representations that can be engineered to be more local and produce more disconnected classification regions. To give an example of a logic system that performs image classification, let us consider the truth table in Figure 1. If input variables $x_{i,j}$ are pixels in a binary image and output c_k are categories, this table represents a multi-class classification task on binary images. The task of learning a classifier can be cast as finding a system of propositions that capture the true table. Given the complexity of the task, it is reasonable to expect propositions to be expressed in terms of subconcepts which, in turn, are expressed by subconcepts until we reach the sensory input:

$$\begin{aligned} \text{class}_1 &\leftarrow \text{concept}_1 \vee \text{concept}_2 \\ \text{class}_2 &\leftarrow (\text{concept}_2 \wedge \text{concept}_4) \vee \text{concept}_3 \\ \dots & \\ \text{concept}_k &\leftarrow (x_{0,0} \wedge x_{0,1}) \vee (\neg x_{0,1} \wedge x_{1,1} \wedge x_{1,2}) \\ \dots & \end{aligned}$$

The alternating pattern of ANDs and ORs that can be seen above is essential for expressiveness. Together, they form

¹Vrije Universiteit, Amsterdam, Netherlands. Correspondence to: Minh Le <m.n.le@vu.nl>.

disjunctive normal forms (DNF) which, when organized into a hierarchy, can express an exponential number of cases. The hierarchical organization of concepts closely resembles CNNs and it can easily be shown that ReLU activation can approximate AND and OR gates.

Although the relationship between neural networks and logical gates was known since the early days of the field (Rojas, 1996), training a deep neural network to resemble a logic function has remained difficult. In the current research, we hypothesize that *it is possible to train deep neural networks to resemble soft hierarchical logic systems and this helps alleviate fooling and adversarial examples*.

The contributions of the current research are as follows:

- We present an alternative perspective on the working of deep neural networks and propose alternative architectures inspired by logic.
- We put forward an alternative interpretation of regularization in ReLU-like networks and propose a new type of regularization.
- We show that it is possible to train an innately local neural network that performs well on MNIST.
- We present new empirical data about the effect of different network designs on robustness against adversarial perturbation and formulate a new explanation for the phenomenon.

In the next sections, we will present the modifications we made (Section 2), experimental procedures (Section 3) and the results (Section 4). Finally, we situate our research in the existing literature (Section 5) and offer some concluding remarks (Section 6).

2. Approximating Propositional Logic in Neural Networks

The process of emulating propositional logic in a high-dimensional space carries with it inherent difficulty. To balance learnability and capacity, we start with ReLU-based CNNs and make amendments where they deviate from the ideals. The results are captured in this section as a series of re-considerations.

2.1. Rethinking Activation Functions

When we think of each neuron as representing a logic formula, constraints must be placed on its range of activation. Common sense suggests that a soft logic function increases when more supporting evidence accumulates but only to a certain point. In other words, it must exhibit a saturation region.

To strike a balance between fidelity and learnability, we introduce the rectified logarithm function (Figure 2a):

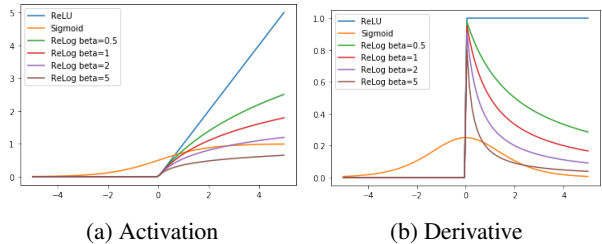


Figure 2. Comparing ReLog with two popular activation functions

$$\text{ReLog}(z; \beta) = \frac{1}{\beta} \log(\beta \max(z, 0) + 1), \quad (1)$$

where $\beta > 0$.

As can be seen in Figure 2b, in the right half of the function, the derivative of ReLog stays meaningful for a much larger range than the sigmoid function.

2.2. Rethinking Neurons

In the standard distributed representations framework, the individual neuron does not carry any particular meaning (Hinton et al., 1986). In contrast, a logical view considers the neuron as a logic formula that evaluates as true for a particular pattern and false for everything else.

Consider the patterns depicted in Figure 3a, which can be captured by:

$$\begin{aligned} y_1 &= x_1 \wedge x_2 \\ y_2 &= (x_1 \wedge x_2) \vee (-x_1 \wedge x_2) \end{aligned}$$

The conjunctions and disjunctions in the above formulae can be implemented in a real-valued realm with min and max. We, therefore, propose MinMaxOut units, a generalization of maxout (Goodfellow et al., 2013) in which incoming input is first passed through a min operation (representing AND) and then a max operation (representing OR):

$$\text{MinMaxOut}_{m,n}(x) = \max_{i=1}^m \min_{j=1}^n \sum_{k=1}^p w_{ijk} x_k \quad (2)$$

The result is a better fit as illustrated in Figure 3b. However, parts of the space are still incorrectly admitted. Considering that, in real applications, we need to fit patterns in high-dimensional space instead of a 2D plane, the problem becomes even harder because the number of linear units needed to fit a Gaussian cloud increases linearly with the number of dimensions.

The second improvement attempts to draw curved boundaries around the data by applying the kernel trick (Bishop,

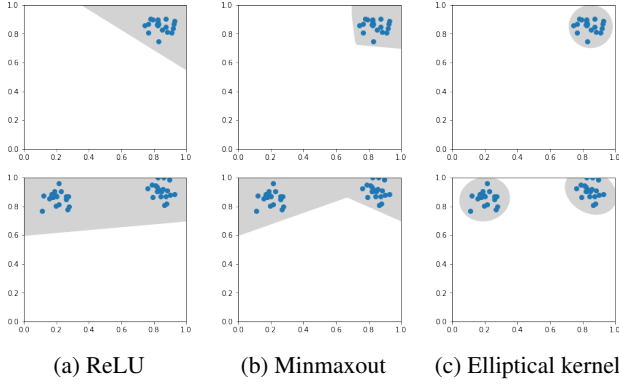


Figure 3. Different types of neurons differ in the ability to fit to the shape of the data.

2006) to the net input of a neuron:

$$z = \sum_{i=1}^m w'_i x_i^2 + \sum_{i=1}^m w_i x_i + b, \quad (3)$$

To create elliptical boundaries, in particular, we use the constraint $w'_i \leq 0 \forall i = 1, \dots, m$. Elliptical units eliminate the need for MinOut but not MaxOut units as illustrated in Figure 3c.

2.3. Rethinking Regularization

Explicit weight regularization is a way to reduce overfitting. This is clear in the textbook case of fitting a polynomial curve where smaller weights can reign in curvature and reduce the degree of the polynomial (Bishop, 2006). However, it is not obvious if and how this translates to a ReLU-based neural network that is linear almost everywhere (?). We argue that smaller weights can either decrease or *enhanced* fitting, depending on the bias.

The distance between a ReLU unit’s decision boundary and a training example in Cartesian space is:

$$d = \frac{|\sum_{i=1}^m w_i x_i + b|}{\sqrt{\sum_{i=1}^m w_i^2}} \quad (4)$$

Similar to a support vector machines (SVM), the margin between the decision boundary and the closest example can be increased by minimizing $\|w\|$ (Bishop, 2006). Notice that, different from SVM, only accepted patterns count because rejected ones lead to zero activation.

On the other hand, the decision boundary is removed from the coordinate origin by:

$$d_0 = \frac{|b|}{\sqrt{\sum_{i=1}^m w_i^2}}. \quad (5)$$

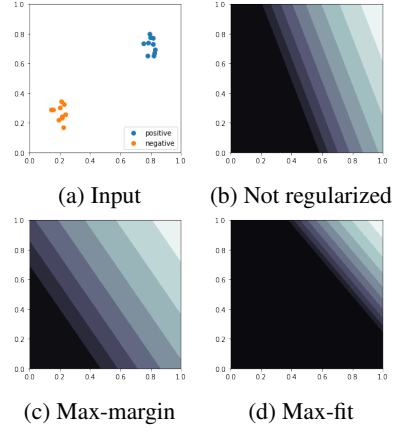


Figure 4. Fitting a ReLU unit to a pattern on 2D plane: the input (a), contour plots of the trained ReLU unit when no regularization is used (b), and when max-margin (c) or max-fit (d) is applied. Black denotes zero-activation; the lighter the color, the stronger the activation.

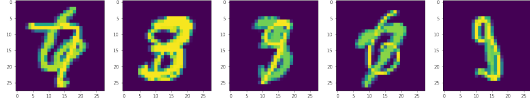


Figure 5. Negative examples used to train our models.

If $b \geq 0$, meaning the accepted input pattern is on the same side as the origin, reducing b would tighten the fit around the pattern. If $b < 0$, the pattern is on the opposite side of the origin, subtracting from b would push the decision boundary further from the origin towards the pattern, therefore having a similar tightening effect.

Taken together, we could identify two ways to regularize a ReLU unit that we shall call max-margin and max-fit (Figure 4):

$$r_{\text{max-margin}} = \frac{\gamma}{m} \sum_{i=1}^m w_i^2, \quad (6)$$

and

$$r_{\text{max-fit}} = \frac{\gamma'_1}{m} \sum_{i=1}^m w_i^2 + \gamma'_2 b \quad (7)$$

where $\gamma, \gamma'_1, \gamma'_2 \in \mathbb{R}^+$ govern the strength of regularization and m is the number of inputs. Similar formulae can be defined for Hamiltonian space (L_1).

2.4. Rethinking Training

Our approximation would not be complete without the ability to compute zero rows in a truth table as in Figure 1. We replace softmax with independent sigmoid activation and train directly on fooling examples. This has been tried in Bromley & Denker (1993) to enhance rejection of so-called “rubbish class” examples.

Because techniques to generate fooling examples are out of the scope of the current paper, we only experimented with overlaying two images from different classes (Figure 5). The images can be efficiently generated from training examples as a data augmentation step.

3. Experimental Design

Experiments were designed to validate the following hypotheses about a model that combines all the proposed modifications:

H1 (learnability and expressiveness): the model can be trained to the same accuracy on a clean dataset.

H2 (locality): the model’s decision boundaries (i.e. regions in input space that a class is predicted with a certainty above a given threshold) are bounded and smaller than a ReLU network.

H3 (validity): trained only on natural examples and augmented ones, the model achieves a higher accuracy on adversarial examples compared to a ReLU network.

It is straightforward to compare models on clean and adversarial examples. To detect locality, we use an interpolation between an image from the test set of MNIST and a uniform noise pattern. The expectation is that a distributed model is strongly activated everywhere while a local model is only strongly activated in the vicinity of a valid pattern while resting at chance level elsewhere.

We also perform ablation analyses to detect the benefit of each proposed trait. Our experiments were executed on two standard datasets using models of different depths and a suite of diverse attacks.

3.1. Datasets

MNIST (Lecun et al., 1998) is a widely used dataset in image recognition. It contains 28×28 gray-scale images of hand-written Arabic digits, divided into 60,000 examples for training and 10,000 for testing. The small scale enables fast experimentation and therefore it is commonly used to evaluate proofs of concept.

CIFAR-10 (Krizhevsky, 2009) contains slightly larger (32×32) color images of 10 classes of objects in natural settings. There are 50,000 training and 10,000 testing examples. Compared to the previous dataset, CIFAR-10 is harder to crack in both natural and adversarial settings.

3.2. Models

For MNIST, we experimented with a simple model with two convolutional layers (16 and 32 channels, both with 5×5 kernels) and a dense connection output layer. This model and its derivatives are trained using Adam (Kingma & Ba, 2015) with learning rate 0.001 for 20 epochs. The

data augmentation methods that we used include random resizing, erasing, rotation, and adding Gaussian noise ($\sigma = 0.3$).

For CIFAR-10, we use a scaled-down version of VGG architecture (Simonyan & Zisserman, 2014) with 8 convolutional layers. This choice helps provide insights into how our method works in a deeper architecture while being lightweight enough for quick experimentation. All models in this line are trained using mini-batch SGD with learning rate 0.01 for 80 epochs. For data augmentation, we make use of random cropping, horizontal flipping, rotation, and Gaussian noise ($\sigma = 0.5$, added after normalization).

3.3. Training with Quadratic and Logarithmic Units

The learnability of ReLU networks roots in their piece-wise linearity whereas architectures with highly non-linear elements are very hard to train. We observe that a vanilla implementation of quadratic and ReLog models has a tendency to oscillate around chance level from the start of training or decrease substantially in performance midway through. To achieve training stability, we start by training a ReLU network and gradually ramp up non-linear elements.

We note that linear functions are simply quadratic functions with second-degree coefficients set to zero. Therefore, to train quadratic units (Section 2.2), we replace Equation 2.2 with:

$$z = \alpha_t \sum_{i=1}^m w'_i x_i^2 + \alpha_t \gamma + \sum_{i=1}^m w_i x_i + b, \quad (8)$$

where t is training step, $\alpha_t \in [0, 1]$, and $\gamma > 0$. The term $\alpha_t \gamma$ is added to the net input to compensate for a possible increase in negativity coming from quadratic terms. Because gradient only flows through active units, gaining new active units is a smaller concern than losing existing ones. For a network initialized with Kaiming method (He, 2015), we find that $\gamma = \sqrt{m}$ is sufficient to stabilize learning.

Similarly, ReLog activation function (Section 2.1) is a generalization of ReLU in the sense that the former approaches the latter when β tends to 0. We, therefore, compute the activation of a neuron as:

$$y = \text{ReLog}(z; \alpha'_t \beta) \quad (9)$$

where α'_t grows by each training step from 0 to 1.

Many hyperparameters are involved in the various models. For practical reasons, we only tried a few combinations that make intuitive sense and select the best one w.r.t. performance on natural datasets.

3.4. Attacks

The importance of evaluating against robust attacks has been highlighted more than once in the literature (Athalye

et al., 2018; Uesato et al., 2018). We use Cleverhans (Papernot et al., 2018), a library of standard implementations of state-of-the-art attacks. Among the algorithms offered there, we selected a battery of attacks from different categories: single-step: **FGM** (Goodfellow et al., 2014); iterative: **BIM** (Kurakin et al., 2017a) and **C&W** (Carlini & Wagner, 2017); gradient-free: **SPSA** (Uesato et al., 2018).

For each combination of attack, model, and dataset, we evaluate on batches of 100 test examples, using between 15 and 100 batches depending on the speed of the attack (SPSA is the slowest, taking more than 3 hours to finish a batch). The accuracy on batches is used to calculate average performance and p -value.¹

4. Results

In this section, we will present experimental results aiming at validating hypotheses laid out in Section 3.

4.1. Learnability and Expressiveness

The performance of our models on clean MNIST digits can be found in Table 2. It is clear that we can reach similar levels of performance with the proposed architecture. When mean squared error is used as a loss function, however, we notice that the performance is significantly lower, and adding negative examples exacerbates the issue.

Training a deep elliptical network is considerably harder. We find that in order to train a modified 8-convolutional-layer network to the same performance as a ReLU-based one, we have to limit α_t to below 0.5 or limit the application of elliptical units to only the first hidden layer. We evaluated both solutions and the latter proves more performant.

To confirm that filters are actually quadratic, we look at the magnitude of quadratic weights. The median of them is 0.0103, larger than 0.0019 of linear weights. Next, we calculate the radii of filters in the first hidden layer along input dimensions. On normalized CIFAR-10 images with intensity values ranging between -2.43 and 2.75, we find 50% of radii to be smaller than 57.52 and 25% of them are smaller than 12.88.

The *Clean* column in Table 3 presents the performance of our models on clean CIFAR-10 images. A trend similar to that of the MNIST experiment is observed: the switch from a piece-wise non-linear function to a highly non-linear one does not hurt performance but the change of training loss and examples have a strong negative effect. A possible explanation is a propositional theory of CIFAR-10 might be excessively big and a more expressive form of logic might be needed. Alternatively, a neural network might need more

¹We use the function `ttest_ind` in SciPy package with `equal_var=False`.

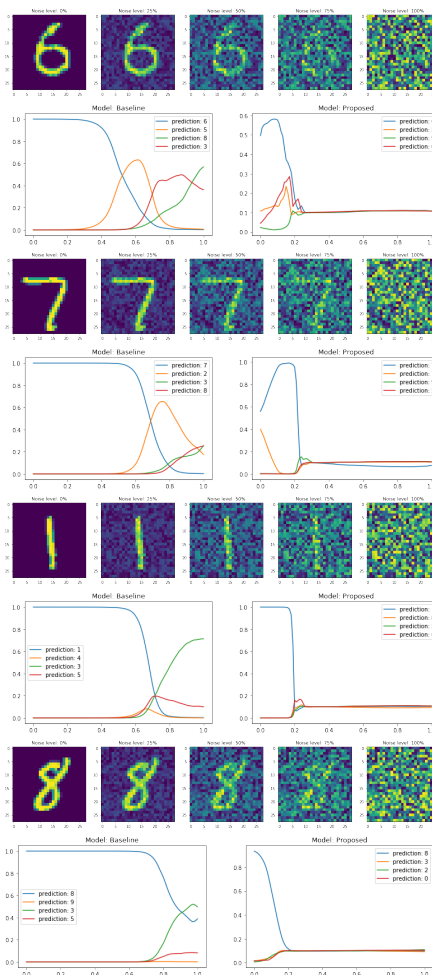


Figure 6. Comparing activation patterns of ReLU and the proposed architecture on noisy images. Horizontal axis: level of noise, vertical axis: softmax activation.

capacity to represent such a propositional theory.

4.2. Locality

Figure 6 depicts the activation pattern of the baseline model (Row 0 in Table 2) and the model with all logic-inspire traits enabled (Row 7 in Table 2). We plot the softmax-normalized probability of four classes selected to include the highest activation for either the given example or the noise pattern.

It can be clearly seen that, whereas the ReLU model emits high probabilities for both true digits and noise, the proposed model is only activated around the test instances. The boundary of around 20% noise might bear some relation to the data augmentation technique we use, with a further boundary being possible if a stronger source of noise is added to training examples. Notice that noise was not used as negative examples, therefore the source of the behavior is in the inductive bias of the technique itself.

Model	Acc.	Model	Acc.
Baseline	0.28	Elliptical+MaxOut	0.03
ReLog	0.06	MaxFit	0.48
MaxOut	0.05	MF.+Elliptical	0.00
MinMaxOut	0.02	MF.+E.+MaxOut	0.79
Elliptical	0.01	MF.+E.+MaxOut+ReLog	1.00
MSE	0.03	MSE+Negative ex.	1.00

Table 1. Performance on the task of classifying noise pattern. Predictions with a softmax score smaller than 0.5 are considered correct.

To evaluate the behavior quantitatively, we run models through 10,000 uniform noise images. Any prediction with higher than 50% confidence is labeled as an error. We isolate the minimum set of traits that enables high robustness to noise by adding one modification at a time. The results presented in Table 1 demonstrate that there are two possible routes: innate and learned.

The innate route trains a model that is inherently local. Applying max-fit on a ReLU network increases the robustness but it still accepts more than half of the noise. An innately local model only emerges when we combine several traits together: elliptical units that are able to focus on a bounded region of the input space, max-fit regularization to tighten this region, and max-out activation to allow the network to model disconnected patterns, therefore focus more on each pattern individually. ReLog enhances the robustness further by mapping accepted patterns to a small range of activation, therefore permitting smaller ellipsoids in the next layer.

In contrast, in the learned route, one uses both normal and negative examples during training. The result in Table 1 shows that this route can also be highly effective. This corroborates with the results of Bromley & Denker (1993) and Nguyen et al. (2015).

On CIFAR-10, our modifications (Row 5, Table 3, i.e. excluding negative examples) increase the chance of rejecting noise from 0% to 5.30% and reduce the prediction confidence on noise from 0.93 (std=0.12) to 0.79 (std=0.16). This result suggests that the model is slightly more local than a ReLU network. The negatively trained model (Row 7) is more robust but at the cost of low accuracy and low confidence on true images. On average, it produces predictions with a probability of 0.21 (std=0.10) on test images and 0.16 (std=0.01) on noise patterns.

4.3. Robustness on MNIST

Table 2 presents the robustness of our models against various attacks. It is clear that the proposed architectures lead to a significant increase in robustness across many types of threats. Since all of our models are trained on standard back-propagation, it is unlikely that this improvement comes from

gradient obfuscation (Athalye et al., 2018). There are other signs that this is not the case: single-step attacks (variants of FGM) and gradient-free attack (SPSA) are generally not more effective than iterative gradient-based attacks (C&W and BIM).

One of the leading hypotheses about the origins of adversarial examples states that it is the local linearity of ReLU models that enable attacks via tiny perturbation (Goodfellow et al., 2014). This hypothesis is compatible with the observation that ReLog is more robust than ReLU against adversarial perturbation. However, it is contradicted by the observation that elliptical units do not lead to improvement on four out of five measures when it replaces min-out.

The connectedness hypothesis (Nguyen et al., 2018) would predict an improvement associated with max-out because of its ability to produce disconnected regions. This is supported by our results.

However, both hypotheses are incomplete in the sense that they cannot explain why max-out only has a minor impact on robustness while min-out increases performance as much as four times.

Based on our analysis in Section 2.2, we hypothesize that the proposed models improve robustness by minimizing the volume of the input region that a neuron accepts in the subspace of active input dimensions. Because any active neuron in a ReLU-like network supports the flow of gradient, the size of the positive region is directly linked to the attack surface that an adversary can exploit. According to this hypothesis, min-out works better than max-out and bare ReLU because it can represent convex polytopes that fit better to input patterns. Elliptical units do not work better on most attacks despite being non-linear everywhere, perhaps because the patterns being modeled (patches of binary images) do not assume a Gaussian distribution. Although max-fit (Row 5) does not get any best results, it does improve the robustness of an elliptical model (Row 4) on two of five counts and maintain statistically equivalent performance on two others.

Training with mean-square error has a mixed effect on robustness. Adversarial examples are an inherently local phenomenon. The effect of activation suppression in distant areas to the decision boundary around an example is a poorly-understood area and beyond the scope of the current paper.

4.4. Robustness on CIFAR-10

Table 3 shows that the proposed architecture succeeds in promoting robustness – all of the best results on adversarial images belong to one of our proposed models.

As max-out leads to overfitting this time, its poor performance on adversarial examples might be a reflection of its

Logic-inspired Deep Neural Networks

Model	Clean	FGM	FGM	C&W	BIM	SPSA
		$\epsilon_\infty = 0.3$	$\epsilon_{L_2} = 2$			
0 Baseline	0.99	0.10	0.71	0.05	0.00	0.16
1 + ReLog ($\beta = 2$)	0.99	0.37*	0.85*	0.23*	0.03*	0.44*
2 + MaxOut ($k = 4$)	0.99	0.40*	0.85	0.23	0.04	0.42
3 + MinOut ($k = 2$)	0.99	0.67*	0.91*	0.32*	0.17*	0.46*
4 + Elliptical	0.96*	0.56*	0.71*	0.59*	0.07*	0.34*
5 + MaxFit (L_1)	0.97*	0.53*	0.75*	0.67*	0.07	0.33
6 + MSE training	0.97*	0.35*	0.79*	0.33*	0.07*	0.37*
7 + Negative examples	0.94*	0.03*	0.26*	0.84*	0.00*	0.01*

Table 2. Accuracy of models on MNIST on different attacks. Elliptical units eliminate the need of MinOut so we disable MinOut from step 4 onward. BIM: iterations=5, C&W: iterations=50, SPSA: iteration=50. An asterisk (*) signifies that the result is statistically significantly different from the previous one on the same column.

Model	Clean	FGM	FGM	CW	BIM
		$\epsilon_\infty = 0.3$	$\epsilon_{L_2} = 2$		
0 Baseline	0.75	0.08	0.42	0.00	0.01
1 + ReLog	0.74*	0.17*	0.44*	0.03*	0.01
2 + MaxOut ($k = 4$)	0.66*	0.13*	0.34*	0.01*	0.00*
3 + MinOut ($k = 2$)	0.72*	0.21*	0.38*	0.03*	0.01*
4 + Elliptical	0.75*	0.18*	0.42*	0.04*	0.01*
5 + MaxFit (L_1)	0.77*	0.20*	0.45*	0.05	0.02
6 + MSE training	0.68*	0.15*	0.36*	0.04*	0.01*
7 + Negative examples	0.43*	0.14*	0.21*	0.04	0.01

Table 3. Accuracy of models on CIFAR-10 on different attacks. BIM: iterations=5, C&W: iterations=50. Elliptical units are applied to the first hidden layer only. An asterisk (*) signifies that the result is statistically significantly different from the previous one on the same column.

poor performance overall instead of its robustness. Min-out succeeds in reigning overfitting and achieves the best performance on FGM, $\epsilon_\infty = 0.3$.

Different from the MNIST experiment, elliptical units yield positive improvements when they replace min-out in the first hidden layer. This observation fits our expectation because natural images tend to display Gaussian distributions which can be better modeled by elliptical curves. The fitting is enhanced further by max-fit, leading to the best performance in three out of four measures. These results support our hypothesis that it is the fit of individual neurons to the patterns passed to them that determines robustness.

The performance of mean square error training is low overall due to learnability issues (see Section 4.1).

5. Related Work

The current research is related to several topics: neural network design, defending models against fooling and adversarial examples, and the integration of neural networks and logic.

5.1. Neural Network Design

The empirical success of deep neural networks in recent years has spurred an extensive literature on network design and all elements of neural networks have been subjected to revision (Soria-Olivas et al., 2003; de Brébisson & Vincent, 2015; Rodrigues & Member, 2017; He et al., 2016, among others).

Some elements of what we proposed here had been introduced in isolation and with a different motivation. As noted in Section 2.4, training with mean squared error and negative examples were already used in Bromley & Denker (1993) to encourage the rejection of “rubbish class” examples. Maxout units were designed by Goodfellow et al. (2013) to facilitate and improve on dropout. Different from our proposal, max-out was originally intended to replace rectified linear units instead of working together with them. Quadratic units were hypothesized in Goodfellow et al. (2014) to improve robustness. Finally, parallel to our research, Fan & Wang (2019) succeeded in training quadratic units and Liu et al. (2019) proposed logarithmic activation functions. Their formulations are slightly different from ours and lack the smooth transition from ReLU.

5.2. Adversarial Examples

Adversarial examples have received a lot of attention since its discovery by [Szegedy et al. \(2013\)](#). Two lines of research may be discerned: one attempts to prove the (im)possibility of defending against adversarial examples and another tries to explain and alleviate them.

The papers in the first line include [Fawzi et al. \(2018\)](#); [Tsipras et al. \(2018\)](#); [Gilmer et al. \(2018\)](#); [Bubeck et al. \(2018\)](#); and [Schmidt et al. \(2018\)](#), which point out some families of models that are incapable of achieving robust high performance or require too many training examples, or too much time, to get there. The majority of the literature, however, has taken a more optimistic view, putting forward hypotheses about the origins of adversarial examples and proposing remedies.

[Goodfellow et al. \(2014\)](#) conjecture that it is the local linearity of ReLU networks that enable attacks. Following this reasoning, [de Alfaro \(2018\)](#) and [Taghanaki et al. \(2019\)](#) show that using radial basis functions (RBFs) as a replacement for ReLU can reduce the success rate of attacks. However, RBFs are not only non-linear but also inherently local and the authors did not test which of these properties is the cause of the improvement.

Results that link robustness to sparseness ([Guo et al., 2018](#)) and margin ([Croce et al., 2018](#); [Wu & Yu, 2019](#); [Galloway et al., 2018](#)) is closely related to the hypothesis advanced in this paper. Similarly, [Mustafa et al. \(2019\)](#) propose to fortify a model by disconnecting classification regions, a hypothesis we started with. Their solutions involve adding a regularization term and therefore can be incorporated into many models, including ours.

Approaches that make use of adversarial examples during training are so far the most successful. They can be classified into two groups: offline generation ([Kurakin et al., 2017b](#)) and modeling an adversary ([Madry et al., 2017](#); [Na et al., 2018](#); [Wong & Kolter, 2018](#)). These approaches are orthogonal to ours.

5.3. Fooling Examples

The concept of “rubbish class” examples was explored more than two decades ago ([Bromley & Denker, 1993](#)). [Nguyen et al. \(2015\)](#) re-popularized this concept under the name “fooling examples” and address the targeted case where an adversary searches for a fooling image that causes prediction in a predetermined class.

Relatively little work was done in addressing fooling examples. An exception is ? which uses an autoencoder with a mixture of Gaussian prior to detect and reject fooling examples.

5.4. Logic

Neural-symbolic integration has been researched for a long time ([Garcez et al., 2015](#)). Early results explore the relative computational power of sigmoid-activated networks and boolean circuits ([Maass et al., 1994](#)) and equivalence between neural networks and logic ([Jang & Sun, 1993](#); [McCulloch & Pitts, 1943](#)), among other topics. More recently, [Hitzler et al. \(2004\)](#) proof that feed-forward neural networks can approximate certain logic semantic operators.

On the empirical side, much work has been done on extracting rules from neural networks, typically motivated by interpretability. ([Towell & Shavlik, 1993](#); [Setiono, 1997](#); [D’Avila Garcez et al., 2001](#); [Hruschka & Ebecken, 2006](#)). Alternatively, [D’Avila Garcez & Gabbay \(2004\)](#) apply neural networks to the problem of learning logical rules.

We do not aim at pursuing the integration of connectionist and symbolic approaches but hope to provide new empirical data for the field.

6. Conclusions

In this paper, we take a logic-inspired view on deep neural networks. By wide-ranging modifications of a standard ReLU architecture and a new training scheme, we create models that produce more local, disconnected representations and is more robust to fooling and adversarial examples.

We count among our main contributions empirical data about the behavior of neural networks on fooling and adversarial examples. First, we illustrate two routes to local models: innate and trained – both lead to more accurate rejection of random noise patterns but with different trade-offs. Second, regarding the defense against adversarial examples, we present empirical results that contradict the popular linearity hypothesis ([Goodfellow et al., 2014](#)). In light of the results, we put forward a hypothesis that links adversarial examples to the size of the patterns that individual neurons accept.

In deep learning research, there seems to be a theory-practice gap between, on the one hand, the predominant theory for explaining the expressiveness of deep neural networks that is based on distributed representations (?) and, on the other hand, numerous papers that study patterns recognized by individual neurons (????). It is unclear where deep neural networks lie in the localist-distributed spectrum or whether there is a spectrum at all. By proposing architectures that resemble logic propositions and a transition from a conventional ReLU architecture, we hope to contribute to the resolution of this issue and better understanding of the inner-workings of deep neural networks.

References

- Athalye, A., Carlini, N., and Wagner, D. Obfuscated gradients give a false sense of security: Circumventing defenses to adversarial examples. *35th International Conference on Machine Learning, ICML 2018*, 1:436–448, 2018.
- Bader, S. and Hitzler, P. Dimensions of Neural-symbolic Integration - A Structured Survey. 2005.
- Bishop, C. M. *Pattern Recognition and Machine Learning*, volume 4 of *Information science and statistics*. Springer, 2006. ISBN 9780387310732. doi: 10.1117/1.2819119.
- Bromley, J. and Denker, J. S. Improving Rejection Performance on Handwritten Digits by Training with Rubbish. *Neural Computation*, 5(3):367–370, 1993. doi: 10.1162/neco.1993.5.3.367.
- Bubeck, S., Price, E., and Razenshteyn, I. Adversarial examples from computational constraints. pp. 1–19, 2018.
- Carlini, N. and Wagner, D. Towards Evaluating the Robustness of Neural Networks. *Proceedings - IEEE Symposium on Security and Privacy*, pp. 39–57, 2017. ISSN 10816011. doi: 10.1109/SP.2017.49.
- Croce, F., Andriushchenko, M., and Hein, M. Provable Robustness of ReLU networks via Maximization of Linear Regions. 2018.
- D’Avila Garcez, A. S. and Gabbay, D. M. Fibring neural networks. *Proceedings of the National Conference on Artificial Intelligence*, pp. 342–347, 2004. doi: 10.1007/978-3-540-73246-4_9.
- D’Avila Garcez, A. S., Broda, K., and Gabbay, D. M. Symbolic knowledge extraction from trained neural networks: A sound approach. *Artificial Intelligence*, 125 (1-2):155–207, 2001. ISSN 00043702. doi: 10.1016/S0004-3702(00)00077-1.
- de Alfaro, L. Neural Networks with Structural Resistance to Adversarial Attacks. pp. 1–19, 2018.
- de Brébisson, A. and Vincent, P. An Exploration of Softmax Alternatives Belonging to the Spherical Loss Family. pp. 1–9, 2015.
- Fan, F. and Wang, G. Fuzzy logic interpretation of quadratic networks. *Neurocomputing*, sep 2019. ISSN 09252312. doi: 10.1016/j.neucom.2019.09.001.
- Fawzi, A., Fawzi, H., and Fawzi, O. Adversarial vulnerability for any classifier. *Advances in Neural Information Processing Systems*, 2018-Decem(NeurIPS):1178–1187, 2018. ISSN 10495258.
- Ford, N., Gilmer, J., Carlini, N., and Cubuk, D. Adversarial Examples Are a Natural Consequence of Test Error in Noise. 2019.
- Galloway, A., Tanay, T., and Taylor, G. W. Adversarial Training Versus Weight Decay. pp. 1–15, 2018.
- Garcez, A. d., Besold, T. R., Raedt, L. d., Földiák, P., Hitzler, P., Icard, T., Kühnberger, K.-U., Lamb, L. C., Miikkulainen, R., and Silver, D. L. Neural-Symbolic Learning and Reasoning: Contributions and Challenges. *AAAI Spring Symposium 2015*, pp. 18–21, 2015. ISSN 03649059. doi: 10.1109/48.922792.
- Gilmer, J., Metz, L., Faghri, F., Schoenholz, S. S., Raghu, M., Wattenberg, M., and Goodfellow, I. The Relationship Between High-Dimensional Geometry and Adversarial Examples. 2018.
- Goodfellow, I., Warde-Farley, D., Mirza, M., Courville, A., and Bengio, Y. Maxout Networks. In *Proceedings of The 30th International Conference on Machine Learning*, pp. 1319–1327, 2013.
- Goodfellow, I. J., Shlens, J., and Szegedy, C. Explaining and Harnessing Adversarial Examples. pp. 1–11, 2014.
- Guo, Y., Zhang, C., Zhang, C., and Chen, Y. Sparse DNNs with improved adversarial robustness. *Advances in Neural Information Processing Systems*, 2018-Decem(NeurIPS): 242–251, 2018. ISSN 10495258.
- He, K. Delving Deep into Rectifiers : Surpassing Human-Level Performance on ImageNet Classification. In *Proceedings of the IEEE international conference on computer vision*, pp. 1026–1034, 2015.
- He, K., Zhang, X., Ren, S., and Sun, J. Deep Residual Learning for Image Recognition. In *Proceedings of the IEEE conference on computer vision and pattern recognition*, pp. 770–778, 2016. ISBN 008036148X.
- Hinton, G. E., McClelland, J. L., and Rumelhart, D. E. Distributed representations. In *Parallel distributed processing*, pp. 77–109. 1986.
- Hitzler, P., Hölldobler, S., and Seda, A. K. Logic programs and connectionist networks. *Journal of Applied Logic*, 2 (3):245–272, 2004. ISSN 15708683. doi: 10.1016/j.jal.2004.03.002.
- Hochreiter, S., Bengio, Y., Frasconi, P., and Schmidhuber, J. Gradient Flow in Recurrent Neural Nets : The Difficulty of Learning Long-Term Dependencies. *A Field Guide to Dynamical Recurrent Neural Network*, pp. 401–403, 2001. ISSN 1098-6596. doi: 10.1109/9780470544037.ch14.

- Hruschka, E. R. and Ebecken, N. F. F. Extracting rules from multilayer perceptrons in classification problems : A clustering-based approach. 70:384–397, 2006. doi: 10.1016/j.neucom.2005.12.127.
- Jang, J.-S. R. and Sun, C.-T. Functional Equivalence Between Radial Basis Function Networks and Fuzzy Inference Systems. 4(9204538):156–159, 1993.
- Kingma, D. P. and Ba, J. Adam: A Method for Stochastic Optimization. In *ICLR 2015*, 2015.
- Krizhevsky, A. Learning Multiple Layers of Features from Tiny Images. 2009. ISSN 00012475.
- Kurakin, A., Goodfellow, I., and Bengio, S. Adversarial examples in the physical world. *ICLR 2017*, 2017a.
- Kurakin, A., Goodfellow, I. J., and Bengio, S. Adversarial machine learning at scale. pp. 1–17, 2017b.
- Lecun, Y., Bottou, L., Bengio, Y., and Haffner, P. Gradient-based learning applied to document recognition. *Proceedings of the IEEE*, 1998.
- Liu, Y., Zhang, J., Gao, C., Qu, J., and Ji, L. Natural-Logarithm-Rectified Activation Function in Convolutional Neural Networks. pp. 1–9, 8 2019.
- Maass, W., Schnitger, G., and Sontag, E. D. A Comparison of the Computational Power of Sigmoid and Boolean Threshold Circuits. *Theoretical Advances in Neural Computation and Learning*, pp. 127–151, 1994. doi: 10.1007/978-1-4615-2696-4{_}.4.
- Madry, A., Makelov, A., Schmidt, L., Tsipras, D., and Vladu, A. Towards Deep Learning Models Resistant to Adversarial Attacks. pp. 1–28, 2017. URL <http://arxiv.org/abs/1706.06083>.
- McCulloch, W. S. and Pitts, W. H. A logical calculus of the ideas immanent in nervous activity. In *Bulletin of mathematical biophysics*, volume 5, pp. 115–133. 1943. ISBN 9781351487214. doi: 10.1007/BF02478259.
- Montúfar, G., Pascanu, R., Cho, K., and Bengio, Y. On the number of linear regions of deep neural networks. *Advances in Neural Information Processing Systems*, 4 (January):2924–2932, 2014. ISSN 10495258.
- Moosavi-Dezfooli, S. M., Fawzi, A., Fawzi, O., and Frossard, P. Universal adversarial perturbations. In *Proceedings - 30th IEEE Conference on Computer Vision and Pattern Recognition, CVPR 2017*, volume 2017-Janua, pp. 86–94, 2017. ISBN 9781538604571. doi: 10.1109/CVPR.2017.17.
- Mustafa, A., Khan, S., Hayat, M., Goecke, R., Shen, J., and Shao, L. Adversarial Defense by Restricting the Hidden Space of Deep Neural Networks. 2019.
- Na, T., Ko, J. H., and Mukhopadhyay, S. Cascade adversarial machine learning regularized with a unified embedding. *ICLR*, pp. 1–16, 2018.
- Nguyen, A., Yosinski, J., and Clune, J. Deep Neural Networks are Easily Fooled: High Confidence Predictions for Unrecognizable Images. In *Proceedings of the IEEE Conference on Computer Vision and Pattern Recognition*, pp. 427436, 2015. ISSN 15573001. doi: 10.1080/04580630600872547.
- Nguyen, Q., Mukkamala, M. C., and Hein, M. Neural networks should be wide enough to learn disconnected decision regions. *35th International Conference on Machine Learning, ICML 2018*, 9:6001–6011, 2018.
- Papernot, N., Faghri, F., Carlini, N., Goodfellow, I., Feinman, R., Kurakin, A., Xie, C., Sharma, Y., Brown, T., Roy, A., Matyasko, A., Behzadan, V., Hambardzumyan, K., Zhang, Z., Juang, Y.-L., Li, Z., Sheatsley, R., Garg, A., Uesato, J., Gierke, W., Dong, Y., Berthelot, D., Hendricks, P., Rauber, J., and Long, R. Technical Report on the CleverHans v2.1.0 Adversarial Examples Library. *arXiv preprint arXiv:1610.00768*, 2018.
- Raghu, M., Poole, B., Kleinberg, J., Ganguli, S., and Dickstein, J. S. On the expressive power of deep neural networks. *34th International Conference on Machine Learning, ICML 2017*, 6:4351–4374, 2017.
- Rodrigues, M. R. D. and Member, S. Robust Large Margin Deep Neural Networks. 65(16):4265–4280, 2017.
- Rojas, R. *Neural networks - A systematic introduction*. 1996. doi: 10.1016/j.neunet.2009.11.007.
- Schmidt, L., Talwar, K., Santurkar, S., Tsipras, D., and Madry, A. Adversarially robust generalization requires more data. *Advances in Neural Information Processing Systems*, 2018-Decem(NeurIPS):5014–5026, 2018. ISSN 10495258.
- Setiono, R. Extracting rules from neural networks by pruning and hidden-unit splitting. *Neural Computation*, 9(1): 205–225, 1997.
- Simonyan, K. and Zisserman, A. Very Deep Convolutional Networks for Large-Scale Image Recognition. pp. 1–14, 2014.
- Soria-Olivas, E., Martín-Guerrero, J. D., Camps-Valls, G., Serrano-López, A. J., Calpe-Maravilla, J., and Gómez-Chova, L. A low-complexity fuzzy activation function for artificial neural networks. *IEEE Transactions on Neural*

Networks, 14(6):1576–1579, 2003. ISSN 10459227. doi: 10.1109/TNN.2003.820444.

Szegedy, C., Zaremba, W., Sutskever, I., Bruna, J., Erhan, D., Goodfellow, I., and Fergus, R. Intriguing properties of neural networks. pp. 1–10, 2013.

Taghanaki, S. A., Abhishek, K., Azizi, S., and Hamarneh, G. A Kernelized Manifold Mapping to Diminish the Effect of Adversarial Perturbations. pp. 11340–11349, 2019.

Towell, G. G. and Shavlik, J. W. Extracting Refined Rules from Knowledge-Based Neural Networks. *Machine Learning*, 13:71–101, 1993.

Tsipras, D., Santurkar, S., Engstrom, L., Turner, A., and Madry, A. Robustness May Be at Odds with Accuracy. pp. 1–24, 2018.

Uesato, J., O’Donoghue, B., Van Den Oord, A., and Kohli, P. Adversarial risk and the dangers of evaluating against weak attacks. *35th International Conference on Machine Learning, ICML 2018*, 11:7995–8007, 2018.

Wong, E. and Kolter, J. Z. Provable defenses against adversarial examples via the convex outer adversarial polytope. *35th International Conference on Machine Learning, ICML 2018*, 12:8405–8423, 2018.

Wu, K. and Yu, Y. Understanding Adversarial Robustness: The Trade-off between Minimum and Average Margin. pp. 1–22, 2019.